SPARSE TOUCH SENSING FOR CAPACITIVE TOUCH SCREENS

Chenchi (Eric) Luo[*], *James McClellan*[*]

Center for Signal and Image Processing
Georgia Institute of Technology

Milind Borkar, *Arthur Redfern*

Systems and Applications R&D Center
Texas Instruments

ABSTRACT

Improved capacitive touch screen responsiveness can be achieved at the expense of the touch screen controller analog hardware complexity and power consumption. This paper proposes a compressive sensing based approach to exploit the sparsity of simultaneous touches (e.g., 10 or less per person) with respect to the number of sensor nodes (e.g., 100s) to achieve similar levels of responsiveness with lower levels of analog complexity and power consumption. This is done by showing that the number of measurements required for touch detection is related to the number of touches rather than the number of nodes.

Index Terms— compressive sensing, capacitive touch screens

1. INTRODUCTION

Capacitive touch screens[1] are used for smartphones, tablets, track pads and kiosks. Trends towards larger screen sizes coupled with battery power limitations place increasing demands on the touch screen controller performance.

Improved capacitive touch screen responsiveness can be achieved at the expense of the touch screen controller analog hardware complexity and power consumption. This paper proposes a compressive sensing based approach to exploit the sparsity of simultaneous touches (e.g., 10 or less per person) with respect to the number of sensor nodes (e.g., 100s) to achieve similar levels of responsiveness with lower levels of analog complexity and power consumption. This is done by showing that the number of measurements required for touch detection is related to the number of touches rather than the number of nodes.

Figure 1 shows the typical structure of a capacitive touch screen. Two layers of indium tin dioxide (ITO) electrodes are laid over a LCD screen. A layer of dielectric material (usually made of plastic or pyrex glass) is located between the two layers of electrodes.

Consider a touch screen layout with M row electrodes and N column electrodes, such that there are MN capacitance sensors or nodes with a parasitic capacitance $\overline{C}$ at the intersection of each column and row electrode. A finger close to a node shunts a portion of the electrical field to ground, which is equivalent to adding a capacitance ΔC in parallel with $\overline{C}$. Therefore, the sensed capacitance on the node becomes $C = \overline{C} + \Delta C$.

Each node on the touch screen can be viewed as a pixel in an image. After calibrating $\overline{C}$ out of C, the remaining ΔC on each node effectively constitutes a 2D image of touches. Touches can be detected as peaks in the image with properties such as finger size, shape, orientation and pressure reflected in the shapes of the peaks. Assuming a small number of fingers relative to number of nodes, the image is sparse and it is possible to develop compressive sensing based approaches to touch sensing.

This paper is organized as follows. Section 2 describes a capacitance sensing technique using charge transfer which is adopted in section 3 for the development of a column based sparse touch sensing scheme. Extensions to full panel sparse touch sensing are described in section 4.

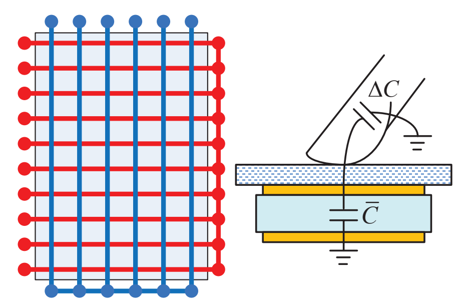

Fig. 1. A typical layout of a capacitive touch screen

2. CAPACITANCE MEASUREMENT BY CHARGE TRANSFER

Charge transfer[2] is a popular method for measuring capacitance on capacitive touch screens. As shown in Figure 2, charge transfer is realized in 2 stages: the pre-charge stage and the transfer stage.

In the pre-charge stage, the unknown capacitor C is charged with a known voltage source V_{drive} such that in

[*]Supported by the Texas Instruments Leadership University grant.

steady state the charge Q is

$$Q = V_{drive} C. \tag{1}$$

In the transfer stage, a known reference capacitor C_{ref} is connected in parallel with C such that the charge on C is transferred onto C_{ref}. Denoting the potential over C_{ref} as V_{sense}, according to the conservation of total charge, we have

$$V_{drive} C = V_{sense}(C + C_{ref}) \tag{2}$$

which can be rearranged as

$$V_{sense} = \frac{C}{C + C_{ref}} V_{drive}. \tag{3}$$

If $C_{ref} \gg C$, we have

$$V_{sense} \approx \frac{C}{C_{ref}} V_{drive} \tag{4}$$

which allows us to estimate the capacitance as a proportional relationship between the drive and sense voltages.

An alternative topology for charge transfer is shown in Figure 3. An operational amplifier is utilized and the polarity of V_{sense} is inverted. This measurement topologies also yield a proportionality relationship between drive and sense voltage as a function of the capacitance:

$$V_{sense} = gCV_{drive} = gQ, \tag{5}$$

where g is a constant.

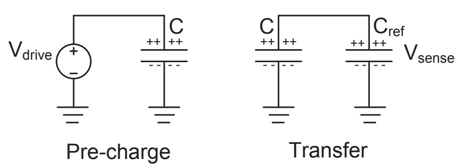

Fig. 2. Charge transfer technique

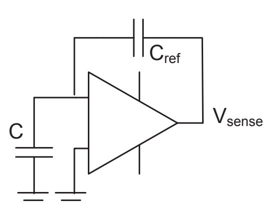

Fig. 3. Alternative charge transfer circuit

3. COLUMN BASED SPARSE TOUCH SENSING

3.1. Setup

Consider a column-wise sensing scheme in which all electrodes in a row are driven with the same voltage in the pre-charge stage, but each row could have a different voltage. In the measurement stage, the charges over each column electrode are converted into a voltage signal in sequential order. The two stage measurement process is repeated K times, each with a distinctive set of row driving voltages.

Now consider the n-th ($n = 0, ..., N-1$) column electrode. Denote $C_{m,n}, m = 0, ..., M-1$ as the node capacitance at the intersection of row m and column n. Also denote the driving voltage at row m for column n during the k-th ($k = 0, ..., K-1$) pre-charge stage as $V_{m,n}^k$. In the transfer stage all the nodes of column n are connected in parallel and the charge accumulated over all n nodes is transferred onto a reference capacitor to induce a sensed voltage:

$$v_n^k = gQ = g \sum_{m=1}^{M} C_{m,n} V_{m,n}^k. \tag{6}$$

Then K measurements can be combined into the following linear equation:

$$\begin{bmatrix} v_n^0 \\ \vdots \\ v_n^{K-1} \end{bmatrix} = g \begin{bmatrix} V_{0,n}^0 & \cdots & V_{M-1,n}^0 \\ \vdots & \ddots & \vdots \\ V_{0,n}^{K-1} & \cdots & V_{M-1,n}^{K-1} \end{bmatrix} \begin{bmatrix} C_{0,n} \\ \vdots \\ C_{M-1,n} \end{bmatrix}. \tag{7}$$

Written in matrix form and ignoring the proportionality constant g we have

$$\mathbf{v}_n = \mathbf{\Phi}_n \mathbf{c}_n, \tag{8}$$

with the following definitions for vectors

$$\mathbf{v}_n = \begin{bmatrix} v_n^0 & \cdots & v_n^{K-1} \end{bmatrix}^T, \tag{9}$$

$$\mathbf{c}_n = \begin{bmatrix} C_{0,n} & \cdots & C_{M-1,n} \end{bmatrix}^T, \tag{10}$$

and for the pre-charge matrix

$$\mathbf{\Phi}_n = \begin{bmatrix} V_{0,n}^0 & \cdots & V_{M-1,n}^0 \\ \vdots & \ddots & \vdots \\ V_{0,n}^{K-1} & \cdots & V_{M-1,n}^{K-1} \end{bmatrix}. \tag{11}$$

The vector $\mathbf{c}_n$ can be recovered from voltage measurements $\mathbf{v}_n$ as long as $\mathbf{\Phi}_n$ is full rank, which requires $K \geq M$, i.e., the number of voltage measurements is not less than the number of nodes on that column. The simplest form of $\mathbf{\Phi}_n$ is an identity matrix, which corresponds to the case where each row is driven sequentially in the pre-charge stage.

3.2. Sparsity of touches

Generally speaking, it is impossible to uniquely recover $\mathbf{c}_n$ from $\mathbf{v}_n$ if $K < M$ because the system of equations would be under-determined. However, if we know that the solution is sparse, $\mathbf{c}_n$ can potentially still be uniquely resolved using compressive sensing[3].

The key assumption is that the number of touches is sparse compared with the number of nodes on the screen.

This assumption can also be extended to each column of nodes, meaning that only a small number of nodes on each column are touched simultaneously.

Denote the parasitic capacitance of column n as

$$\bar{\mathbf{c}}_n = \begin{bmatrix}\bar{C}_{0,n} & \cdots & \bar{C}_{M-1,n}\end{bmatrix}^T. \tag{12}$$

The capacitance changes caused by touches on column n are

$$\Delta\mathbf{c}_n = \mathbf{c}_n - \bar{\mathbf{c}}_n, \tag{13}$$

where $\Delta\mathbf{c}_n$ is assumed to be sparse (i.e., there are only a small number of non-zero entries in $\Delta\mathbf{c}_n$). Combining equations (8) and (13), rearranging terms and defining $\mathbf{v}_n^c$ as the calibrated voltage measurements for column n we can write

$$\mathbf{v}_n^c = \mathbf{v}_n - \mathbf{\Phi}_n\bar{\mathbf{c}}_n = \mathbf{\Phi}_n\Delta\mathbf{c}_n \tag{14}$$

for the case of perfect calibration and

$$\mathbf{v}_n^c = \mathbf{\Phi}_n\Delta\mathbf{c}_n + \mathbf{e}_n \tag{15}$$

for the case of calibration error $\mathbf{e}_n$.

Equation (15) is a classic problem in compressive sensing. If $\mathbf{\Phi}_n$ is an random Gaussian or Bernoulli matrix and $\Delta\mathbf{c}_n$ has a sparsity of s, with $K = O(s\log(M/s))$ measurents $\Delta\mathbf{c}_n$ can be uniquely recovered with an overwhelming probability by solving

$$\min \|\Delta\mathbf{c}_n\|_1 \quad s.t. \quad \|\mathbf{v}_n^c - \mathbf{\Phi}_n\Delta\mathbf{c}_n\|_2 \leq \varepsilon, \tag{16}$$

where ε is a bound for the calibration error.

In practice, it is difficult or costly to implement $\mathbf{\Phi}_n$ as a random Gaussian or Bernoulli matrix. [4] shows that random Toeplitz or circulant matrices are as effective as random matrices. Moreover, these matrices can be easily realized in hardware (e.g., by performing a circular convolution with a random sequence) and permit much faster decoding.

3.3. Large sensor spacing topology

First consider the case of where the distance between each node is much larger than the size of touching objects (e.g., fingers). As a result, a touch object could only induce capacitance changes in nodes in a close vicinity of the touch. For this case $\mathbf{c}_n$ is sparse and can be recovered according to (16).

Figure 4 shows a sensing example with large sensor spacing topology. Each entry in the pre-charge matrix follows a random Bernoulli distribution such that each node is randomly charged with {+V, -V} voltages. Figure 5 shows the recovered $\mathbf{c}_n$ according to (16). In this example a successful recovery is achieved at a compression ratio of 8.

3.4. Small sensor spacing topology

Next consider the case where the distance between each node is small compared with the size of the touching object. As a result, multiple nodes are influenced by a single touch and $\Delta\mathbf{c}_n$ is not sparse in its current form.

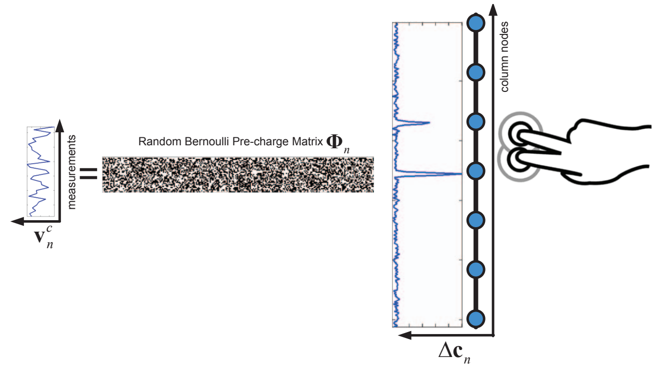

Fig. 4. Large sensor spacing topology: $M = 256, K = 32$

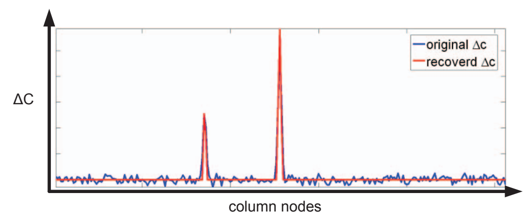

Fig. 5. Recovery with large sensor spacing topology

The key for this case is to find a sparsifying basis $\mathbf{\Psi}$ such that the projection $\boldsymbol{\alpha}_n$ of $\Delta\mathbf{c}_n$ under $\mathbf{\Psi}$ is sparse, and modify the recovery algorithm in (16) to include the sparsifying basis

$$\min \|\boldsymbol{\alpha}_n\|_1 \quad s.t. \quad \|\mathbf{v}_n^c - \mathbf{\Phi}_n\mathbf{\Psi}\boldsymbol{\alpha}_n\|_2 \leq \varepsilon \qquad \Delta\mathbf{c}_n = \mathbf{\Psi}\boldsymbol{\alpha}_n. \tag{17}$$

Figure 5 shows a recovery example of $\Delta\mathbf{c}_n$ under the small sensor spacing topology assumption with a DFT matrix used as the sparsifying matrix $\mathbf{\Psi}$.

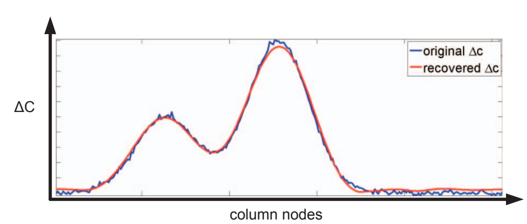

Fig. 6. Recovery with a small sensor spacing topology. $M = 256, K = 32$

For topologies other than the above mentioned cases, it is essential to find an appropriate sparsifying basis. This could be accomplished by either investigating a class of commonly used basis (e.g. DFT, DCT, wavelet, curvelet, etc.) or learning the sparsifying basis from the data with the K-SVD algorithm [5]. Once the sparsifying basis $\mathbf{\Psi}$ is determined, the pre-charge matrix $\mathbf{\Phi}_n$ can be further optimized [6] to minimize the mutual coherence between $\mathbf{\Psi}$ and $\mathbf{\Phi}_n$. As a result, the number of minimally required measurements can potentially be further reduced.

3.5. Constrained optimization

There are two main classes of algorithms used to solve the constrained ℓ_1 optimization problems in (16) and (17): linear/convex optimization [7] and greedy algorithms [8]. Greedy algorithms are attractive in terms of hardware realization due to their computational simplicity.

For this specific problem, two additional characteristics of $\Delta\mathbf{c}_n$ can be exploited. First, the nonnegative assumption of $\Delta\mathbf{c}_n$ leads to a variant of the matching pursuit algorithm in [9] that is guaranteed to find the sparse solution if $\mathbf{\Phi}_n$ is properly designed. Second, for small to medium sensor spacing topologies, the nonzero entries in $\Delta\mathbf{c}_n$ will be clustered in the vicinity of the touch points instead of sporadically. Model-based compressive sensing theory [10] can be applied to enhance the recovery algorithm according to this block-wise sparsity characteristic.

4. FULL PANEL SPARSE TOUCH SENSING

The column-wise compressive sparse touch sensing scheme can be easily extended to a full panel sensing scheme using a sensing architecture which is similar to the single pixel camera architecture for compressive imaging[11].

As shown in Figure 7, each node is driven with a controllable voltage source in the pre-charge stage. In the transfer stage, all MN nodes are connected in parallel such that the charges accumulated over each individual node are mixed together and transferred onto a reference capacitor to derive a voltage measurement. Recovery then proceeds in a manner similar to that of the column based case.

The proposed full panel sparse touch sensing scheme is able to minimize the relative sparsity of active touches compared with the total number of sensors. Therefore, the total number of measurements is minimized given the same maximum active touch points assumption.

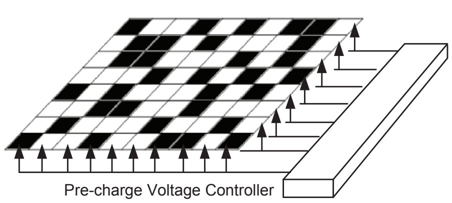

Fig. 7. Full panel compressive sparse touch sensing requires MN voltage drives.

5. REFERENCES

[1] Barret G. and Omote R., "Projected-capacitive touch technology," *Information Display*, vol. 26, no. 3, pp. 16–21, Mar. 2010.

[2] H. Philipp, "Charge transfer sensing," *Sensor Review*, vol. 13, no. 11, pp. 96–105, May 1999.

[3] E.J. Candes and T. Tao, "Near-optimal signal recovery from random projections: Universal encoding strategies?," *Information Theory, IEEE Transactions on*, vol. 52, no. 12, pp. 5406 –5425, Dec. 2006.

[4] H. Rauhut, "Circulant and Toeplitz Matrices in Compressed Sensing," in *SPARS'09 - Signal Processing with Adaptive Sparse Structured Representations*, Rémi Gribonval, Ed., Saint Malo, France, 2009, Inria Rennes - Bretagne Atlantique.

[5] M. Aharon, M. Elad, and A. Bruckstein, "K-SVD: An algorithm for designing overcomplete dictionaries for sparse representation," *Signal Processing, IEEE Transactions on*, vol. 54, no. 11, pp. 4311 –4322, Nov. 2006.

[6] M. Elad, "Optimized projections for compressed sensing," *Signal Processing, IEEE Transactions on*, vol. 55, no. 12, pp. 5695 –5702, Dec. 2007.

[7] M. Grant and S. Boyd, "CVX: Matlab software for disciplined convex programming, version 1.21," `http://cvxr.com/cvx`, Apr. 2011.

[8] D. Needell, J. Tropp, and R. Vershynin, "Greedy signal recovery review," in *Signals, Systems and Computers, 2008 42nd Asilomar Conference on*, Oct. 2008, pp. 1048 –1050.

[9] A.M. Bruckstein, M. Elad, and M. Zibulevsky, "On the uniqueness of nonnegative sparse solutions to underdetermined systems of equations," *Information Theory, IEEE Transactions on*, vol. 54, no. 11, pp. 4813 –4820, Nov. 2008.

[10] R.G. Baraniuk, V. Cevher, M.F. Duarte, and C. Hegde, "Model-based compressive sensing," *Information Theory, IEEE Transactions on*, vol. 56, no. 4, pp. 1982 – 2001, April 2010.

[11] M. B. Wakin, J. N. Laska, M. F. Duarte, D. Baron, S. Sarvotham, D. Takhar, K. F. Kelly, and R. G. Baraniuk, "An architecture for compressive imaging," in *IEEE International Conference on Image Processing*, 2006, pp. 1273–1276.